

Short communication

Synthesis of pure nano-sized $\text{Li}_4\text{Ti}_5\text{O}_{12}$ powder via solid-state reaction using very fine grinding media

Seung-Woo Han, Jin-Wook Shin, Dang-Hyok Yoon*

School of Materials Science and Engineering, Yeungnam University, Gyeongsan 712-749, South Korea

Received 11 May 2012; accepted 22 May 2012

Available online 30 May 2012

Abstract

$\text{Li}_4\text{Ti}_5\text{O}_{12}$ was synthesized by a solid-state reaction using Li_2CO_3 and anatase TiO_2 at 800 °C for 3 h for anode application in Li-ion batteries. In order to examine the effects of milling conditions on the properties of $\text{Li}_4\text{Ti}_5\text{O}_{12}$, 3 different ZrO_2 media of sizes 0.45, 0.10 and 0.05 mm were subjected to 5 h of high energy milling, while 5 mm balls were subjected to 24 h of ball milling for comparison. High energy milling was found to be much more effective in decreasing both the reaction temperature and the final $\text{Li}_4\text{Ti}_5\text{O}_{12}$ particle size than ball milling through the efficient size reduction and mechanochemical activation of the starting materials. The use of 0.10 and 0.05 mm beads resulted in the synthesis of pure nanosized $\text{Li}_4\text{Ti}_5\text{O}_{12}$, depressing the formation of unwanted rutile TiO_2 in the final products, whereby the finer milling media showed more desirable particle properties. Consequently, pure $\text{Li}_4\text{Ti}_5\text{O}_{12}$ of 145 nm size, which is comparable to the particle sizes from expensive wet chemical methods, could be synthesized by an economic solid-state reaction.

© 2012 Elsevier Ltd and Techna Group S.r.l. All rights reserved.

Keywords: A. Milling; A. Powders; solid state reaction; D. Spinel; E. Batteries

1. Introduction

Lithium ion batteries (LIBs) have been extensively studied for high-power applications, such as electric vehicles and large-scaled energy storage systems [1,2]. Even though the current graphite anode material is appropriate for portable electronic devices with good cycle life and moderate capacity (372 mA h/g), it is known to have weaknesses in fast charging properties, power densities and safety issues related to lithium deposition for high power applications [3,4]. In these aspects, a spinel-type lithium titanate ($\text{Li}_4\text{Ti}_5\text{O}_{12}$) is a promising anode material for high power LIBs owing to its high structural stability and capability of fast charging associated with the 3-dimensional network channels for Li^+ diffusion [5–8]. The possible safety problems originating from the deposition of highly reactive lithium metal could also be effectively avoided because it does not form a solid electrolyte interface due to the flat Li insertion potential of 1.55 V (vs. Li/Li^+) [6,9]. In spite of these benefits,

however, $\text{Li}_4\text{Ti}_5\text{O}_{12}$ does not yet meet all the requirements for high power applications due to poor electrical conductivity and slow Li^+ diffusion. In order to improve the rate performance of $\text{Li}_4\text{Ti}_5\text{O}_{12}$, therefore, doping using other metal ions and/or incorporation of highly conductive carbon has been suggested [10,11]. From the kinetic point of view, the synthesis of nanosized $\text{Li}_4\text{Ti}_5\text{O}_{12}$ seems to be most important and could offer a shorter Li^+ diffusion path and greater electrode–electrolyte contact area to enhance the rate properties [12–14].

The most economic $\text{Li}_4\text{Ti}_5\text{O}_{12}$ synthetic method is the solid-state reaction using TiO_2 and Li_2CO_3 followed by heat treatment at 800–900 °C, which generally results in a significant amount of agglomeration along with a coarse particle size. This is why liquid phase synthesis methods such as hydrothermal and coprecipitation have been attempted to decrease the particle size in spite of their high cost [15,16]. Recently, fine ceramic particles could be successfully synthesized via solid-state reaction with the help of newly available very fine starting materials and advanced high energy mills [17,18]. The reduction in particle size with uniform distribution and mechanochemical activation for the starting materials by heavy milling is

*Corresponding author. Tel.: +82 538102561; fax: +82 538104628.

E-mail address: dhyoon@ynu.ac.kr (D.-H. Yoon).

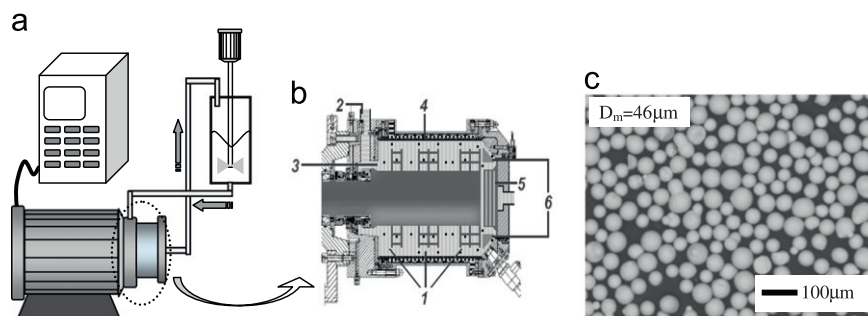


Fig. 1. Schematic of (a) the high energy mill, (b) the enlarged milling chamber with 1: rotor with disks, 2: inlet, 3: milling media, 4: cooling jacket, 5 and 6: separation system, (Web-site of CB Mills Division of Chicago Boiler Company, <http://www.cbmills.com>.) and (c) the ZrO_2 milling medium with $D_m=0.05$ mm. Web-site of CB Mills Division of Chicago Boiler Company, <http://www.cbmills.com>.

a key factor for the decrease in solid-state reaction temperature as well as the final particle size [17–19]. Compared to the conventional ball mills which use a discontinuous operating system, modern high energy mills use a continuous operating system equipped with high speed rotors rotating at up to several thousand rotations per minute (rpm), disk agitators and a cooling system, as shown in Fig. 1. Their high energy input, along with the use of small grinding media with diameters 0.05–0.8 mm, enables the production of very small particles in a short processing time.

With this background, we have examined the effects of high energy milling on $\text{Li}_4\text{Ti}_5\text{O}_{12}$ particle properties using 3 different ZrO_2 media of sizes 0.45, 0.10 and 0.05 mm. Twenty four hours of conventional ball milling was also performed using 5 mm balls for comparison. The evolution of starting material size upon milling as a function of the media size and milling time, and the effects of milling conditions on solid-state reaction temperature as well as the size and purity of synthesized $\text{Li}_4\text{Ti}_5\text{O}_{12}$ were studied. Special attention was paid to the synthesis of pure $\text{Li}_4\text{Ti}_5\text{O}_{12}$ with a particle size ≤ 200 nm by a solid-state reaction for practical applications.

2. Experimental procedure

Coarse Li_2CO_3 ($D_m=4.50$ μm , purity $> 99.5\%$, Shanghai Element International, China) and fine anatase-phased TiO_2 ($D_m=230$ nm, purity $> 99.0\%$, Cosmo Chemical, Korea) were used as Li- and Ti-precursor, respectively. To synthesize 100 g of $\text{Li}_4\text{Ti}_5\text{O}_{12}$ powder, 32.53 g of Li_2CO_3 and 86.84 g of TiO_2 , which corresponds to a Li/Ti stoichiometric ratio of 4.05/5.00, were mixed with 200 g of de-ionized water after adding 2 wt% of the ammonium salt of polycarboxylic acid (Cerasperse 5468-CF, San Nopco, Korea) with respect to the ceramic powder, as a dispersant. This slight excess in Li from the stoichiometric Li/Ti=4/5 was determined based on the preliminary test, considering Li evaporation during the high temperature treatment.

Three batches of slurries were exposed to 5 h of high energy milling (MiniCer, Netzsch, Germany) operated at 3000 rpm using each of 0.45, 0.10 and 0.05 mm ZrO_2

beads, where a small amount of sample was taken at a planned time during the milling for characterization. Twenty four hours of ball milling with 5 mm ZrO_2 balls was also performed using another batch for comparison. After drying the slurries at 100 $^\circ\text{C}$ in a rotary evaporator for uniform mixing, 4 types of mixtures were heat-treated at 800 $^\circ\text{C}$ for 3 h in air at a heating rate of 5 $^\circ\text{C}/\text{min}$.

The morphology of the particles was characterized by a scanning electron microscope (SEM: S-4800, Hitachi, Japan). The mean particle size was estimated from the SEM images by measuring the maximum and minimum diameters of 100 particles using an image analysis software (SigmaScan, Systat Software, USA). The thermal decomposition behaviors of 4 different samples were examined by thermogravimetric analysis (TGA: SDT Q600, TA Instruments, USA) in a flowing air atmosphere at temperatures ranging from room temperature to 800 $^\circ\text{C}$ with a heating rate of 5 $^\circ\text{C}/\text{min}$. Room temperature XRD (RT-XRD: X'Pert-PRO MPD, Panalytical using Cu K_α line, 40 kV and 30 mA) and Rietveld refinement were performed for quantitative phase verification after heat treatment.

3. Results and discussion

According to the SEM images of the starting materials shown in Fig. 2, Li_2CO_3 has a coarse particle size of 4.50 μm , whereas anatase TiO_2 has a relatively fine particle size of 230 nm. Since a solid-state reaction occurs at the contact points of the starting materials, the preparation of very fine and uniformly dispersed Li_2CO_3 and TiO_2 is very important for enhancing the reaction rate and decreasing the processing temperature. Therefore, efficient milling for the starting materials is essential for the synthesis of fine $\text{Li}_4\text{Ti}_5\text{O}_{12}$ particles.

Fig. 3 shows the SEM images of the starting materials after (a) 24 h of ball milling, and 5 h of high energy milling using (b) 0.45, (c) 0.10 and (d) 0.05 mm ZrO_2 beads. The ball-milled sample in Fig. 3(a) still showed coarse Li_2CO_3 particles after 24 h of milling, while the samples that were high energy-milled for 5 h showed fine and uniform particles, as shown in Fig. 3(b)–(d). It was found that the size of the starting materials decreased with the decrease in milling media size. The mean particle sizes were 240, 195

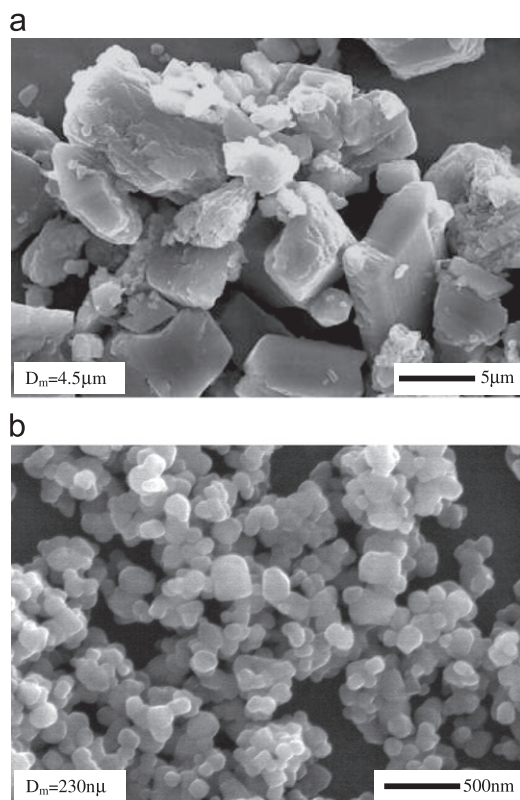


Fig. 2. SEM images of the starting materials: (a) Li_2CO_3 and (b) anatase TiO_2 shown with the mean particle size. Note the different magnifications used for the images.

and 125 nm when 0.45, 0.01 and 0.05 mm media were used, respectively, which are much smaller than that ($D_m = 385 \text{ nm}$) of 24 h of ball milling. Fig. 4 shows the evolution of mean particle size of the starting materials as a function of high energy milling time for 3 different sizes of media. The particle size decreased drastically at the initial milling stage of up to 1 h due to the size reduction of coarse BaCO_3 followed by a mild size reduction upon further milling. The significant milling efficiency of a high energy mill comes from the high shear and collision forces of the small beads generated by the enforced disk rotation at 3000 rpm. On the other hand, the efficiency of ball milling is relatively low because ball milling utilizes the forces generated by gravitation upon the jar rotation at low speed, i.e., 120 rpm in this experiment. Regarding the media size effect of the high energy milling, it is expected that the smaller medium gives better milling efficiency owing to the enhanced chances of collision and shearing to the particles, whereby 0.05 mm beads used in this experiment are the smallest commercially available and introduced recently into the market.

Fig. 5 presents the TGA results for the 4 samples prepared by different milling methods and media sizes, showing drastic weight loss between 300 and 700 $^\circ\text{C}$. Even though the same starting materials were used, a difference in reaction temperature was observed depending on the milling conditions. The high energy-milled samples generally showed lower reaction temperature than that of the

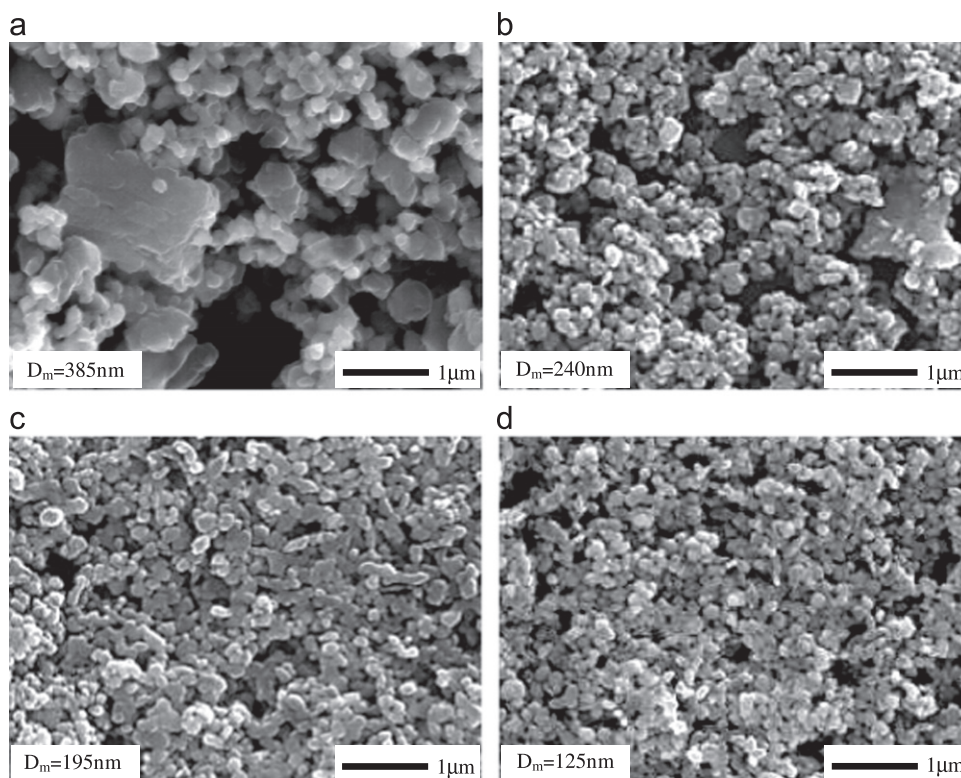


Fig. 3. SEM images of the starting materials after (a) 24 h of ball milling using 5 mm balls, and 5 h of high energy milling using different sizes of ZrO_2 milling media of (b) 0.45, (c) 0.10 and (d) 0.05 mm.

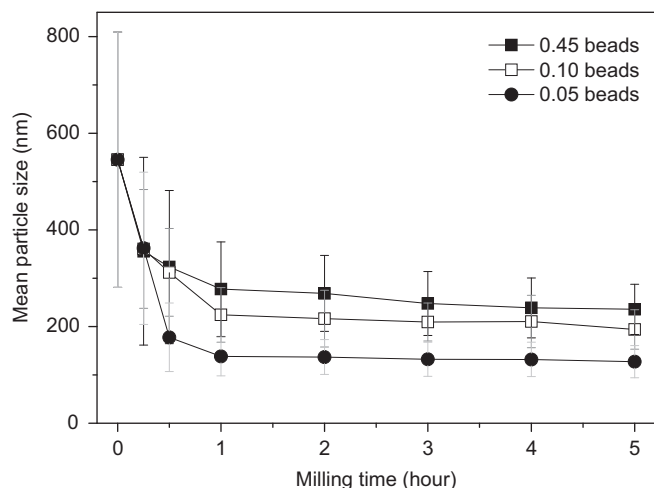


Fig. 4. Evolution of the mean particle size of the starting materials as a function of high energy milling time for the different sizes of ZrO_2 milling media.

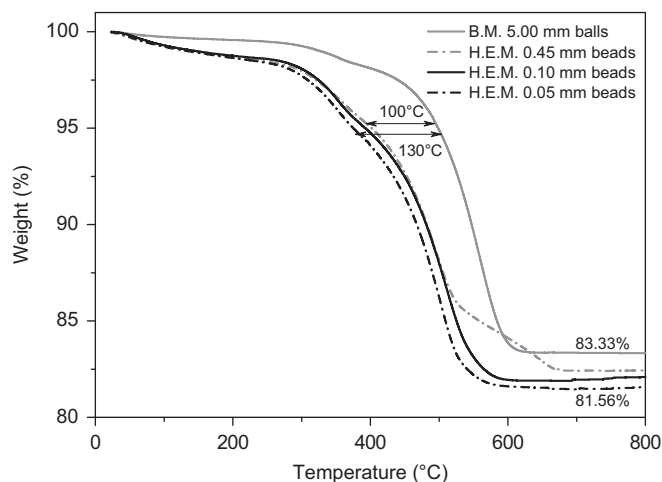


Fig. 5. TGA results for the 4 different samples prepared by different milling methods and media sizes, showing the effect of milling on the solid-state reaction temperature.

ball-milled sample with the maximum gap of 130 °C, as indicated in the figure. In addition, the use of finer media for the high energy milling resulted in lower reaction temperature. This decrease in the reaction temperature by high energy milling can be explained by shortened diffusion length required for the reaction and mechanochemical activation for the starting materials. The greater weight loss of 16.7–18.4% than 16.1%, which is calculated from the solid-state reaction equation $2\text{Li}_2\text{CO}_3 + 5\text{TiO}_2 \rightarrow \text{Li}_4\text{Ti}_5\text{O}_{12} + 2\text{CO}_2$, could be explained by the adsorbed water on the fine starting materials.

Fig. 6 shows the SEM images of the $\text{Li}_4\text{Ti}_5\text{O}_{12}$ powders synthesized by heat treatment at 800 °C for 3 h. The mean particle size of the $\text{Li}_4\text{Ti}_5\text{O}_{12}$ prepared by 24 h of ball milling is 285 nm, while the sizes of those prepared by 5 h of high energy milling are 215, 175 and 145 nm for the media sizes of 0.45, 0.10 and 0.05 mm, respectively. This trend in $\text{Li}_4\text{Ti}_5\text{O}_{12}$ size change upon different

milling conditions is exactly consistent with the starting materials size variation shown in Fig. 3 and the reaction temperature behavior shown in Fig. 5. Therefore, it can be summarized that the more severe milling resulted in finer starting material size which enhances the solid-state reaction at lower temperature and hence decreases the final $\text{Li}_4\text{Ti}_5\text{O}_{12}$ size.

Fig. 7 shows the XRD patterns of 4 different samples heat-treated at 800 °C for 3 h in air. Although most reports used heat treatment at ≥ 800 °C for ≥ 12 h for the solid-state synthesis of $\text{Li}_4\text{Ti}_5\text{O}_{12}$ [7–9,20–27], the samples were kept at 800 °C for only 3 h to examine the effects of milling conditions on $\text{Li}_4\text{Ti}_5\text{O}_{12}$ formation in this test. The XRD pattern of the $\text{Li}_4\text{Ti}_5\text{O}_{12}$ prepared by 24 h of ball milling revealed the existence of Li_2TiO_3 and rutile TiO_2 phase. The small trace peaks for rutile TiO_2 could also be found at 27.5° and 54.2° 2θ for the sample that was high energy-milled using 0.45 mm beads, while those using 0.10 and 0.05 mm beads showed pure $\text{Li}_4\text{Ti}_5\text{O}_{12}$ phase. Since the intermediate Li_2TiO_3 compound is formed when Li is richer than Ti, the presence of this phase for only the 24 h ball-milled sample would be attributed to the incomplete solid-state reaction at 800 °C due to the long diffusion path required for their reaction, by considering the fact that the solid-state reaction occurs through Li^+ diffusion into virgin TiO_2 [28]. The rutile TiO_2 peaks observed for the samples ball-milled and high energy-milled using 0.45 mm beads indicate anatase \rightarrow rutile TiO_2 phase transformation because pure anatase TiO_2 was used as a starting material. It was reported that this transformation occurred from 600 °C under the existence of Li_2CO_3 [29], which is considerably lower than the typical anatase \rightarrow rutile transformation at 900–1000 °C [30–32] due to the catalytic effect of Li_2CO_3 . Moreover, the transformed rutile TiO_2 was known to be very rigid in solid-state reaction, remaining even after heat treatment at 900 °C for 15 h and hindering the formation of pure $\text{Li}_4\text{Ti}_5\text{O}_{12}$ at high temperatures.

This presence of undesired rutile TiO_2 phase in the final $\text{Li}_4\text{Ti}_5\text{O}_{12}$ has been a significant question for the LIB scientific community [33–35]. Since $\text{Li}_4\text{Ti}_5\text{O}_{12}$ for high power applications is believed to work in more severe environments than the electrode materials used in portable electronics, the synthesis of pure fine $\text{Li}_4\text{Ti}_5\text{O}_{12}$ particles is a prerequisite for safety and electrochemical property enhancement purposes. In this aspect, high energy milling using 0.1 and 0.05 mm media seems to offer a solution for the synthesis of pure fine $\text{Li}_4\text{Ti}_5\text{O}_{12}$ particles, as shown in Fig. 7.

Table 1 summarizes the phase content calculated by a Rietveld simulation for 4 different $\text{Li}_4\text{Ti}_5\text{O}_{12}$ particles along with their milling conditions, starting material size, and final particle size after heat treatment at 800 °C for 3 h. It is clear that the high energy milling is much more effective than the conventional ball milling in decreasing the starting material and final $\text{Li}_4\text{Ti}_5\text{O}_{12}$ particle sizes. Moreover, the synthesis of pure $\text{Li}_4\text{Ti}_5\text{O}_{12}$ particles smaller

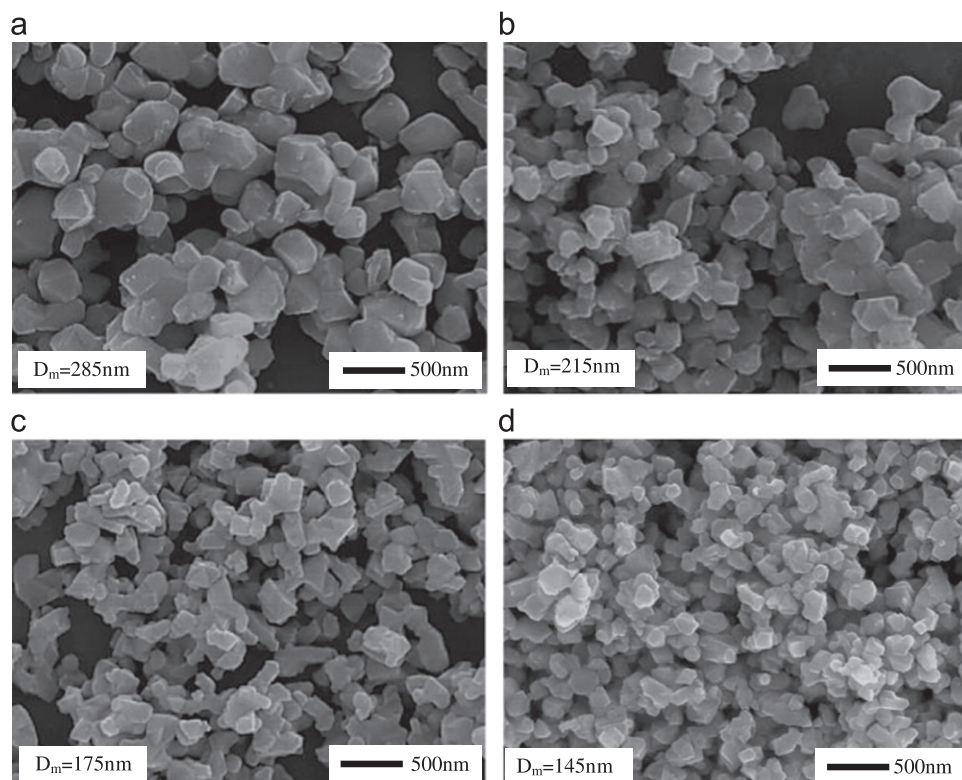


Fig. 6. SEM images of the $\text{Li}_4\text{Ti}_5\text{O}_{12}$ particles heat-treated at 800°C for 3 h after (a) 24 h of ball milling using 5 mm balls, and 5 h of high energy milling using different sizes of ZrO_2 milling media of (b) 0.45, (c) 0.10 and (d) 0.05 mm.

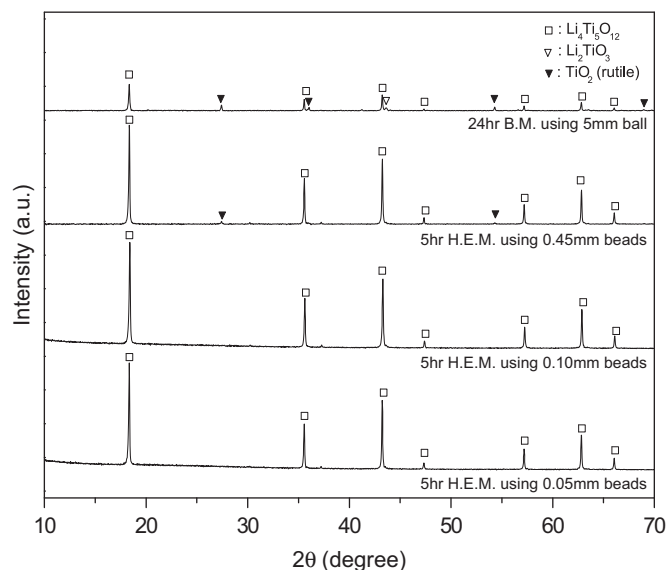


Fig. 7. XRD patterns of the $\text{Li}_4\text{Ti}_5\text{O}_{12}$ samples synthesized using different milling methods and media sizes followed by heat treatment at 800°C for 3 h.

than 200 nm, which is comparable to the particle sizes from expensive wet chemical methods, could be successful by utilizing the very fine 0.10 and 0.05 mm beads associated with the modern high energy milling. Enhanced electrochemical capacity and high rate properties are expected with this nanosized $\text{Li}_4\text{Ti}_5\text{O}_{12}$ due to its pure

Table 1

Starting material size after milling, $\text{Li}_4\text{Ti}_5\text{O}_{12}$ size and phase content after heat treatment at 800°C for 3 h using different milling methods and media sizes.

Type ^a	Milling		Starting material size after milling (nm)	$\text{Li}_4\text{Ti}_5\text{O}_{12}$ size (nm)	Phases (%)		
	Ball size (mm)	Time (h)			$\text{Li}_4\text{Ti}_5\text{O}_{12}$	TiO_2 (rutile)	Li_2TiO_3
B.M.	5.00	24	385	285	90.5	7.7	1.8
H.E.M.	0.45	5	240	215	98.1	1.9	0
	0.10	5	195	175	100	0	0
	0.05	5	125	145	100	0	0

^aB.M.=ball milling, H.E.M.=high energy milling.

phase and fine particle size, which are currently under investigation.

4. Conclusions

The effects of media size for high energy milling on the properties of solid-state reacted $\text{Li}_4\text{Ti}_5\text{O}_{12}$ were examined using 3 different ZrO_2 media with 0.45, 0.10 and 0.05 mm diameters. Twenty four hours of ball milling using 5 mm ZrO_2 balls was also performed for comparison for Li_2CO_3 and anatase-phased TiO_2 starting materials. High energy milling with fine media was shown to be much more effective than the conventional ball milling in acquiring

fine starting materials due to the sufficient collision and shear forces. It was found that sufficient high energy milling for the starting materials could decrease the solid-state reaction temperature more than 100 °C as well as reduce the final $\text{Li}_4\text{Ti}_5\text{O}_{12}$ size down to 145 nm. Moreover, the use of 0.10 and 0.05 mm ZrO_2 beads suppressed the formation of undesired rutile TiO_2 phase owing to the sufficient mechanochemical activation and decreased diffusion length. As a result, 145 nm-sized fine $\text{Li}_4\text{Ti}_5\text{O}_{12}$ particles with 100% purity could be synthesized by an economic solid-state reaction method using high energy milling combined with 0.05 mm medium.

Acknowledgments

This study was supported by the Industrial Core Technology Program funded by The Ministry of the Knowledge Economy, Republic of Korea, (Project no. 10035302).

References

- [1] M. Armand, J.M. Tarascon, Building better batteries, *Nature* 451 (2008) 652–657.
- [2] H. Nishide, K. Oyaizu, Materials science—toward flexible batteries, *Science* 319 (2008) 737–738.
- [3] A.K. Shukla, T.P. Kumar, Materials for next-generation lithium batteries, *Current Science* 94 (2008) 314–331.
- [4] M. Winter, J.O. Besenhard, M.E. Spahr, P. Novak, Insertion electrode materials for rechargeable lithium batteries, *Advanced Materials* (Weinheim, Germany) 10 (1998) 725–743.
- [5] K.M. Colbow, J.R. Dahn, R.R. Haering, Structure and electrochemistry of the spinel oxides LiTi_2O_4 and $\text{Li}_{4/3}\text{Ti}_{5/3}\text{O}_4$, *Journal of Power Sources* 26 (1989) 397–402.
- [6] K. Zaghib, M. Armand, M. Gauthier, Electrochemistry of anodes in solid-state Li-ion polymer batteries, *Journal of the Electrochemical Society* 145 (1998) 3135–3140.
- [7] A. Guerfi, S. Sévigny, M. Lagacé, P. Hovington, K. Kinoshita, K. Zaghib, Nano-particle $\text{Li}_4\text{Ti}_5\text{O}_{12}$ spinel as electrode for electrochemical generators, *Journal of Power Sources* 119–121 (2003) 88–94.
- [8] G. Wang, J. Xu, M. Wen, R. Cai, R. Ran, Z. Shao, Influence of high-energy ball milling of precursor on the morphology and electrochemical performance of $\text{Li}_4\text{Ti}_5\text{O}_{12}$ ball-milling time, *Solid State Ionics* 179 (2008) 946–950.
- [9] K. Hsiao, S. Liao, J. Chen, Microstructure effect on the electrochemical property of $\text{Li}_4\text{Ti}_5\text{O}_{12}$ as an anode material for lithium-ion batteries, *Electrochimica Acta* 53 (2008) 7242–7247.
- [10] P. Kubiak, A. Garcia, M. Womes, L. Aldon, J. Olivier-Fourcade, P. Lippens, J. Jumas, Phase transition in the spinel $\text{Li}_4\text{Ti}_5\text{O}_{12}$ induced by lithium insertion influence of the substitutions Ti/V, Ti/Mn Ti/Fe, *Journal of Power Sources* 119–121 (2003) 626–630.
- [11] H.G. Jung, J. Kim, B. Scrosati, Y.K. Sun, Micron-sized, carbon-coated $\text{Li}_4\text{Ti}_5\text{O}_{12}$ as high power anode material for advanced lithium batteries, *Journal of Power Sources* 196 (2011) 7763–7766.
- [12] G.G. Amatucci, F. Badway, A.D. Pasquier, T. Zheng, An asymmetric hybrid nonaqueous energy storage cell, *Journal of the Electrochemical Society* 148 (2001) A930–A939.
- [13] L. Kavan, J. Procházka, T. Spitler, M. Kalvác, M. Zúkalová, T. Drezen, M. Grätzel, Li insertion into $\text{Li}_4\text{Ti}_5\text{O}_{12}$ —charge capability vs. particle size in thin-film electrodes, *Journal of the Electrochemical Society* 150 (2003) A1000–A1007.
- [14] J. Li, Z. Tang, Z. Zhang, Controllable formation and electrochemical properties of one-dimensional nanostructured spinel $\text{Li}_4\text{Ti}_5\text{O}_{12}$, *Electrochemistry Communications* 7 (2005) 894–899.
- [15] S.Y. Yin, L. Song, X.Y. Wang, M.F. Zhang, K.L. Zhang, Y.X. Zhang, Synthesis of spinel $\text{Li}_4\text{Ti}_5\text{O}_{12}$ anode material by a modified rheological phase reaction, *Electrochimica Acta* 54 (2009) 5629–5633.
- [16] N.A. Alias, M.Z. Kufian, L.P. Teo, S.R. Majid, A.K. Arof, Synthesis and characterization of $\text{Li}_4\text{Ti}_5\text{O}_{12}$, *Journal of Alloys and Compounds* 486 (2009) 645–648.
- [17] S.S. Ryu, D.H. Yoon, Solid-state synthesis of nano-sized BaTiO_3 powder with high tetragonality, *Journal of Materials Science* 42 (2007) 7093–7099.
- [18] D.H. Yoon, Tetragonality of barium titanate powder for a ceramic capacitor application, *Journal of Ceramic Processing Research* 7 (2006) 343–354.
- [19] W.S. Jung, H.S. Park, Y.J. Kang, D.H. Yoon, Lowering the sintering temperature of Gd-doped ceria by mechanochemical activation, *Ceramics International* 36 (2010) 371–374.
- [20] S. Huang, Z. Wen, X. Zhu, Z. Gu, Preparation and electrochemical performance of Ag doped $\text{Li}_4\text{Ti}_5\text{O}_{12}$, *Electrochemistry Communications* 6 (2004) 1093–1097.
- [21] H.E. Park, I.W. Seong, W.Y. Yoon, Electrochemical behaviors of wax-coated Li powder/ $\text{Li}_4\text{Ti}_5\text{O}_{12}$ cells, *Journal of Power Sources* 189 (2009) 499–502.
- [22] G.J. Wang, J. Gao, L.J. Fu, N.H. Zhao, Y.P. Wu, T. Takamura, Preparation and characteristic of carbon-coated $\text{Li}_4\text{Ti}_5\text{O}_{12}$ anode material, *Journal of Power Sources* 174 (2007) 1109–1112.
- [23] S. Huang, Z. Wen, Z. Zhu, Z. Lin, Effects of dopant on the electrochemical performance of $\text{Li}_4\text{Ti}_5\text{O}_{12}$ as electrode materials for lithium ion batteries, *Journal of Power Sources* 165 (2007) 408–412.
- [24] H. Kitauro, A. Hayashi, K. Tadanaga, M. Tatsumisago, High-rate performance of all-solid-state lithium secondary batteries using $\text{Li}_4\text{Ti}_5\text{O}_{12}$ electrode, *Journal of Power Sources* 189 (2009) 145–148.
- [25] B.H. Choi, D.J. Lee, M.J. Ji, Y.J. Kwon, S.T. Park, Study of the electrochemical properties of $\text{Li}_4\text{Ti}_5\text{O}_{12}$ doped with Ba and Sr anodes for lithium-ion secondary batteries, *Journal of the Korean Ceramic Society* 47 (2010) 638–642.
- [26] P.P. Prosini, R.M. Mancini, L. Petrucci, V. Contini, P. Villano, $\text{Li}_4\text{Ti}_5\text{O}_{12}$ as anode in all-solid-state, plastic, lithium-ion batteries for low-power applications, *Solid State Ionics* 144 (2001) 185–192.
- [27] J. Shu, Electrochemical behavior and stability of $\text{Li}_4\text{Ti}_5\text{O}_{12}$ in a broad voltage window, *Journal of Solid State Electrochemistry* 13 (2009) 1535–1539.
- [28] J.W. Shin, C.H. Hong, D.H. Yoon, Effects of TiO_2 starting materials on the solid-state formation of $\text{Li}_4\text{Ti}_5\text{O}_{12}$, *Journal of the American Ceramics Society* 95 (2012) 1894–1900.
- [29] C.H. Hong, A. Noviyanto, J.H. Ryu, J. Kim, D.H. Yoon, Effects of the starting materials and mechanochemical activation on the properties of solid-state reacted $\text{Li}_4\text{Ti}_5\text{O}_{12}$ for lithium ion batteries, *Ceramics International* 38 (2012) 301–310.
- [30] F.C. Gennari, D.M. Pasquevich, Kinetics of the anatase–rutile transformation in TiO_2 in the presence of Fe_2O_3 , *Journal of Materials Science* 33 (1998) 1571–1578.
- [31] P.S. Ha, H.J. Youn, H.S. Jung, K.S. Hong, Y.H. Park, K.H. Ko, Anatase–rutile transition of precipitated titanium oxide with alcohol rinsing, *Journal of Colloid and Interface Science* 223 (2000) 16–20.
- [32] J. Arbiol, J. Cerdà, G. Dezaneeau, A. Cirera, F. Peiró, A. Cornet, J.R. Morante, Effects of Nb doping on the TiO_2 anatase-to-rutile phase transition, *Journal of Applied Physics* 92 (2002) 853–861.
- [33] T. Yuan, R. Cai, R. Ran, Y. Zhou, Z. Shao, A mechanism study of synthesis of $\text{Li}_4\text{Ti}_5\text{O}_{12}$ from TiO_2 anatase, *Journal of Alloys and Compounds* 505 (2010) 367–373.
- [34] E. Matsui, Y. Abe, M. Senna, A. Guerfi, K. Zaghib, Solid-state synthesis of 70 nm $\text{Li}_4\text{Ti}_5\text{O}_{12}$ particles by mechanically activating intermediates with amino acids, *Journal of the American Ceramic Society* 91 (2008) 1522–1527.
- [35] J. Li, Y.L. Jin, X.G. Zhang, H. Yang, Microwave solid-state synthesis of spinel $\text{Li}_4\text{Ti}_5\text{O}_{12}$ nanocrystallites as anode materials for lithium-ion batteries, *Solid State Ionics* 178 (2007) 1590–1594.